Systematic Study of Elastic Scattering of ^{6}Li+^{40}Ca using BDM3Y-Paris and Wood Saxon Potential

Harun Al Rashid*
Department of Physics, BBK College,
Nagaon, Barpeta-781311, India;
Department of Physics,
Gauhati University,
Guwahati-781014, India

Nabendu K. Deb, Lakhyajit Sarma, K. Kalita
Department of Physics,
Gauhati University
Guwahati-781014, India

Mousumi Bhuyan
Department of Physics,
Rangia College,
Rangia-781354, India

Amar Das
Department of Physics, Suren Das College,
Hajo-781102, India; Department of Physics,
Gauhati University
Guwahati-781014, India

***Abstract*—Elastic scattering angular distributions of ^{6}Li from ^{40}Ca in the energy range 20-240 MeV, data available in the literature, have been analyzed. Theoretical calculations have been carried out in the framework of optical model using the code available online at www.nrv.org.ru. Different optical potentials were employed. In the first approach, a double folding potential for the real part and Wood Saxon volume potential for the imaginary part of the interacting nuclear potential was used. BDM3Y-Paris potential is used as a candidate of double folding potential. In the second approach, double folding potential is replaced by Wood Saxon (volume term) whereas the imaginary part is volume Wood Saxon. A comparison between experimental data and present calculations is made and best fit parameters are listed. The energy dependence of Wood Saxon potential parameters is examined.**

Keywords— OM parameters; Double folding; Elastic Scattering

I. INTRODUCTION

Study of elastic scattering is an important part to understand peripheral heavy ion (HI) interaction. Any nuclear interaction involves nuclear potential along with Coulomb potential and the choice of the nuclear potential reveals a wide variety of phenomenon subjected to the fitting percentage with the experimental data. Highly celebrated optical model (OM) formalism allows us to play with different kind of potentials such as Wood-Saxon (WS), Folding, Proximity etc. In Wood-Saxon formalism at least six parameters are varied in order to analyze elastic scattering data and previous experimental results have showed that WS formalism is very good phenomenological model to study nuclear collision. However, great success of WS formalism is shadowed when interaction is observed with very high energetic beam. Though, any HI interaction can be dissected by considering the aspects such as beam energy, charge, mass etc., however more satisfactory understanding is more probabilistic using nucleon-nucleon (NN) interaction potential. To construct nucleus-nucleus potential, integration is carried out over a NN potential over the whole mass distribution of colliding partners. This approach is known as folding and this method has been widely used to generate real part of the OM potential [1-7]. Watanabe first attempted to formulate folding picture of nuclear collision which was further extended successfully by Satchler and Love incorporating NN potential with nucleon densities [8,9].

Last several decades have witnessed that double folding model has been widely used to generate real parts of both alpha nucleus and heavy ion potentials. It is relatively simple model as it uses only first order term of interacting potential [10]. M3Y is a popular choice of NN interaction potentials which generates G matrix elements for the two different forms known as Paris and Reid [11,12]. Double Folding (DF) approach reduces the number of free parameters as compared to WS approach.

In heavy ion collision, with the increasing effect of short range nuclear force, the system moves toward inelastic channel from elastic channel where angular distribution becomes Fresnel type at barrier energy whereas it becomes Fraunhofer type above the Coulomb barrier [13]. Previously, Woods *et al.* have discussed in detail of elastic scattering of lithium from target with A < 24 using double folding potential [14]. In this work, we have we have analyzed elastic cross section of the reaction ^{6}Li+^{40}Ca at energies 20 MeV, 26 MeV, 28 MeV, 30 MeV, 32 MeV, 34 MeV, 88 MeV, 99 MeV, 156 MeV, 210 MeV and 240 MeV. Experimental data of elastic scattering at above mentioned energies are taken from the references [15-22]. Analysis is carried out employing two approaches. In the first approach, real part of the potential is generated using a double folding potential and the imaginary potential is generated using WS potential, whereas in the second approach both real and imaginary nuclear potential is taken to be WS. We obtain unique set of OM parameters from both approaches by comparing the theoretical data with experimental data. Large angle anomaly is observed when we try to fit experimental data at very large angle (more than 100^{0}). We attempt to extract a more generalized set of OM parameters for the reaction ^{6}Li+^{40}Ca so that these parameters can be used for other reactions channels like fusion, transfer etc. Also dependence of parameters on projectile energy is one of the aspects of our study. Theoretical analysis is carried out using an online code available at the website www.nrv.org.ru [23]. Previous studies have showed that phenomenological potentials like WS lacks data at backward angles as well as at higher energies compared to the data obtained by DF potential as WS

potential does not include local interaction of nuclear matter. More or less, WS potential can be applied satisfactorily at low energy for the system ^{6}Li+^{40}Ca, however there is still ambiguities regarding the application of WS potential at higher energies. We examine the applicability of WS as well as DF potential in a wide energy range.

A brief description of theoretical model is given in Sec. II. The calculation and results are presented in Sec. III while we conclude in Sec.IV.

II. OM FORMALISM: BRIEF DESCRIPTION

The present calculations are performed using an OM analysis code that is available online at www.nrv.org.ru. The details of the code and methodology used are described in [24-26]. Here only some details relevant to the present calculations are provided.

The optical potential $V_{tot}(r)$ consists of two parts (i) Nuclear potential and (ii) Coulomb potential:

$$V_{total}(r) = V_{Nuc}(r)+V_{Coul}(r) \quad (1)$$

The Coulomb part of the potential (V_{Coul}) has the form

$$V_{Coul}(r) = \begin{cases} \frac{1}{4\pi\varepsilon_0}\frac{Z_P Z_T e^2}{r}, r \geq R_C \\ \frac{1}{4\pi\varepsilon_0}\frac{Z_P Z_T e^2}{2R_C}(3-\frac{r^2}{R_C^2}), r \leq R_C \end{cases} \quad (2)$$

where, Z_P and Z_T corresponds to charge number of the projectile and target, respectively. R_C is Coulomb radius and is calculated as $R_C = r_{OC}(A_P^{1/3}+A_T^{1/3})$ with r_{OC} = 1.3 fm [27] where A_P and A_T are masses of the projectile and the target. OM calculations are not very much sensitive to Coulomb radius parameter; hence we have kept fixed the value at 1.3 fm in this study. The nuclear part of the potential consists of real and imaginary parts, however no spin-orbit and tensor dependent terms were included as the present version of the code does not have that provision. In our present analysis, the real part of nuclear potential, $V_{Nuc}(r)$, has chosen as either Double Folding or WS potential and the imaginary part always WS.

In the first approach, we used the M3Y-Paris [11, 12] double folding potential which has the following form

$$v_{NN}(r) = \left(11062\frac{e^{-4r}}{4r} - 2538\frac{e^{-2.5r}}{2.5r} + F_{ex}(E)\delta(r)\right) MeV \quad (3)$$

The third term within the parentheses provides the effect of anti-symmetrization in knock-on exchange reaction. For M3Y interaction this term is given by

$$F_{ex}(E) \approx J_{ex}(1-\tau E/A)\ \text{MeV. fm}^3 \quad (4)$$

where the parameters in Paris form of the potential are J_{ex} = -590 and τ = 0.002.

The double folding potential can be obtained by integrating over the volume of the projectile and target nuclei [8,9]

$$V_F(r) = \iint \rho_1(r_1)\rho_2(r_2)v_{NN}(r-r_1+r_2)d^3r_1 d^3r_2 \quad (5)$$

where $\rho_1(r_1)$ and $\rho_2(r_2)$ are the nuclear matter densities of the projectile and target nucleus. As M3Y potential is assumed to have only radial dependence, so heavy ion interaction potential can be expressed as multiplication of two independent terms: one containing the radial dependence term, i.e. v_{NN} (r) and the other being the density and energy dependent form factor, f(ρ,E).

$$V(r,\rho,E) = f(\rho,E)\, v_{NN}(r) \quad (6)$$

As detailed in [28-35], we used the BDM3Y form of density dependence and is written as

$$f(\rho) = C(1-\gamma\rho^{\lambda}) \quad (7)$$

where the parameters for the present system are C = 1.2521 and γ = 1.7452 and $\rho = \rho_1(r_1)+\rho_2(r_2)$. The nuclear and charge densities of the projectile and the target nuclei are calculated using the two parameter Fermi-type function (Fermi 2p)

$$\rho_{p,n}(r) = \rho_{0_{p,n}}\left[1+\exp\left(\frac{r-R_{p,n}}{a_{p,n}}\right)\right]^{-1} \quad (8)$$

where $R_{p,n} = r_{p,n}A^{1/3}$ is the proton (p) or neutron (n) distribution radius, whereas $r_{p,n}$ and $a_{p,n}$ are radius and diffuseness parameter. For ^{6}Li, $r_{p,n}$ = 0.55 fm and $a_{p,n}$ = 0.534 fm, whereas for ^{40}Ca, $r_{p,n}$ = 1.012 fm and $a_{p,n}$ = 0.464 fm [32, 35].

The imaginary part of the potential was taken as WS type which has the following form

$$V_N(r) = \frac{-V_0}{1+\exp(\frac{r-R_{0R}}{a_R})} + i\frac{-W_0}{1+\exp(\frac{r-R_{0I}}{a_I})} \quad (9)$$

$R_0 = r_0 (A_P^{1/3}+A_T^{1/3})$ where A_P and A_T are masses of projectile and target respectively. V_0, R_{0R} and a_R are real depth, radial distance and diffuseness parameters respectively; whereas W_0, R_{0I} and a_I are corresponding imaginary terms. An overall normalization factor N_R was introduced for the DF potential. The normalization factor and WS potential parameters were varied in order to get best agreement between the calculated and measured angular distribution data.

In the second approach of analysis of elastic scattering cross section, WS form (volume term) of the optical potential as given in (9) was used for both real and imaginary parts. Total six parameters are varied in this approach to reproduce experimental angular distribution which is discussed in the following section.

III. CALCULATIONS AND RESULTS

Theoretical analysis is carried out using the code available at the website www.nrv.jinr.ru. The website provides user to calculate elastic cross-section and has provision to compare the data with available experimental data.

TABLE I. OM PARAMETERS EXTRACTED FROM ELASTIC SCATTERING ANALYSIS OF ^{6}Li+^{40}Ca AT VARIOUS BEAM ENERGIES. REAL PART OF INTERACTING POTENTIAL IS BDM3Y-PARIS TYPE OF WHICH N_R IS ADJUSTABLE FACTOR, WHEREAS IMAGINARY PART OF THE POTENTIAL IS WS TYPE (VOLUME)

Energy (MeV)	N_R	W_0 (MeV)	r_{0I} (fm)	a_{0I} (fm)	Type
20	1.45	30	1.1	0.65	Paris+WS Vol.
26	1.36	39	1.1	0.65	Paris+WS Vol.
28	1.35	40	1.1	0.65	Paris+WS Vol.
30	1.30	43	1.1	0.65	Paris+WS Vol.
32	1.28	48.1	1.1	0.65	Paris+WS Vol.
34	1.25	50	1.1	0.65	Paris+WS Vol.
88	0.955	50	1.0	0.881	Paris+WS Vol.
99	0.933	55	1.002	0.884	Paris+WS Vol.
156	0.90	57	1.0	0.811	Paris+WS Vol.
210	1.1	55	1.0	0.884	Paris+WS Vol.
240	1.1	60	1.0	0.811	Paris+WS Vol.

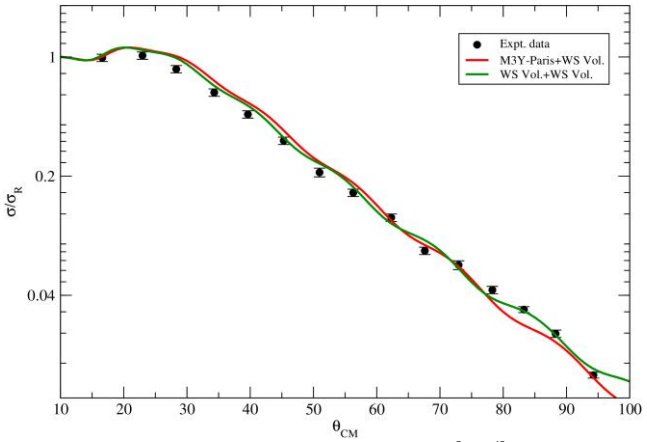

Fig. 1 The elastic scattering angular distribution of ^{6}Li+^{40}Ca reaction at 20 MeV using BDM3Y-Paris and WS potentials are compared with the experimental data. In the plot, black dots are experimental data points. Experimental data are taken from [15]

To extract the OM parameters for ^{6}Li+^{40}Ca, first we employ the first method as discussed above where we vary real N_R along with imaginary parameters, W_0, r_{0I} and a_{0I} of WS volume potential for the energy range 20 MeV-240 MeV.

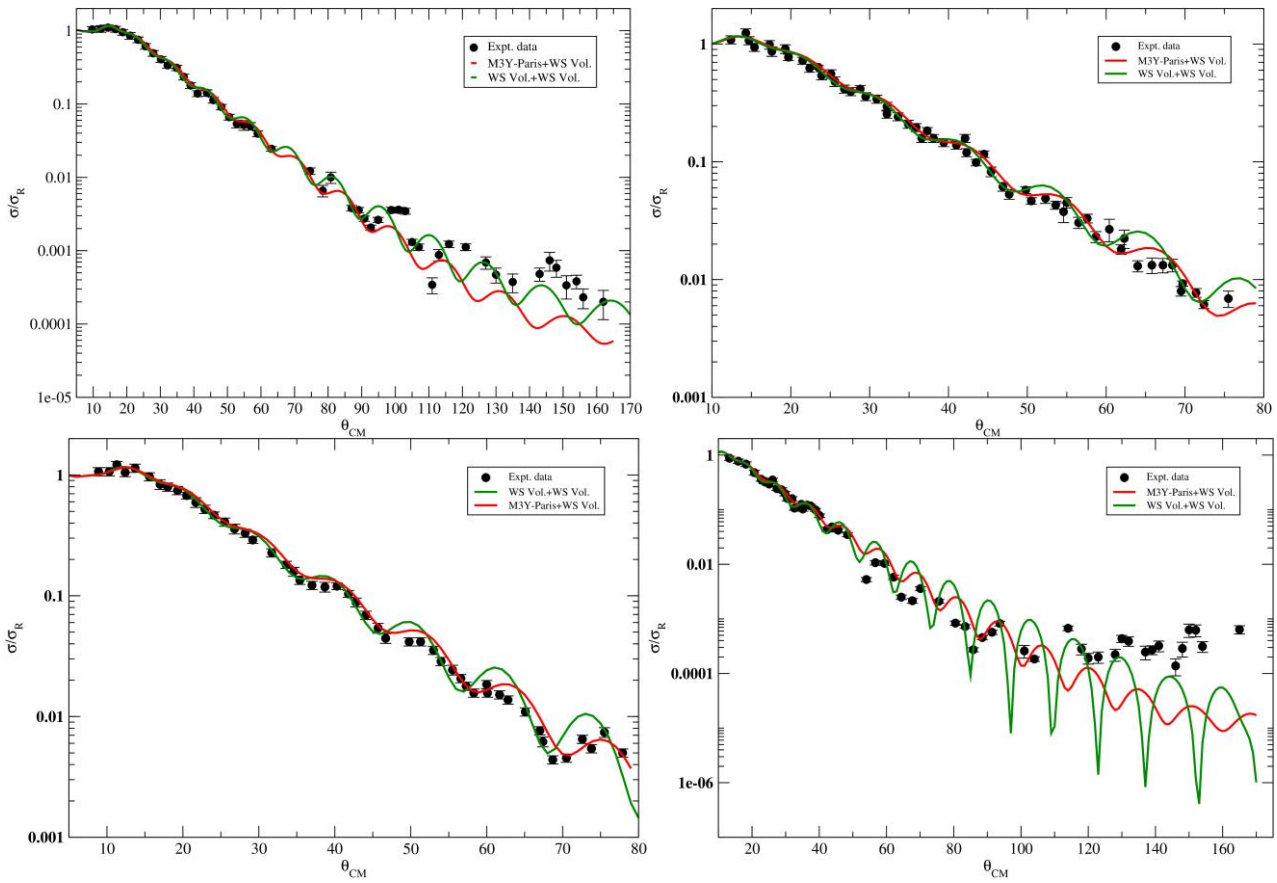

Fig. 2 The elastic scattering angular distribution of ^{6}Li+^{40}Ca reaction at 26 MeV (upper left), 28 MeV (upper right), 30 MeV (lower left) and 34 MeV (lower right) using BDM3Y-Paris and WS potentials are compared with the experimental data. In the plot, black dots are experimental data points. Experimental data are taken from [16]

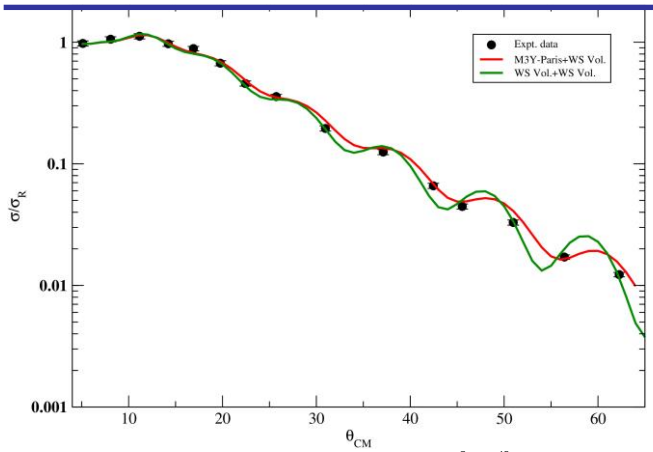

Fig. 3 The elastic scattering angular distribution of ^{6}Li+^{40}Ca reaction at 32 MeV using BDM3Y-Paris and WS potentials are compared with the experimental data. In the plot, black dots are experimental data points. Experimental data are taken from [17]

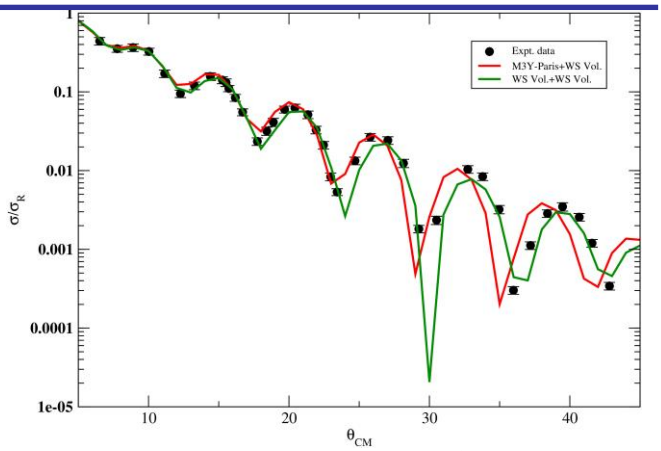

Fig. 5 The elastic scattering angular distribution of ^{6}Li+^{40}Ca reaction at 99 MeV using BDM3Y-Paris and WS potentials are compared with the experimental data. In the plot, black dots are experimental data points. Experimental data are taken from [19]

For the energy range 20 MeV-34 MeV, radius and diffuseness parameters are kept fixed at 1.1 fm and 0.65 fm whereas WS imaginary depth, W_0 and real N_R are varied in order to reproduce experimental elastic angular distribution. Keeping the radius and diffuseness parameters fixed for small energy difference enables us to carry out a systematic investigation of variation of real N_R and imaginary WS depth with incident energy. However, radius and diffuseness parameters are varied to 1.0 fm and around 0.811 fm for large energy range 88 MeV-240 MeV. The extracted OM parameters are listed in Table 1. From the table it is clear that at higher energies, diffuseness parameter is large compared to that at lower energies which indicates the opening of more and more inelastic channels at higher energies. N_R shows gradual decrement with increase of energy whereas imaginary depth shows the opposite nature.

Then, real DF potential is replaced by WS volume potential whereas the imaginary part is kept WS volume same as before. Overall six parameters are varied in this approach. However, radius and diffusion parameters are fixed at 1.1 fm and 0.63 fm both for real and imaginary potential for incident energies of 20 MeV to 34 MeV. These parameters are varied at energies 88 MeV, 99 MeV, 156 MeV, 210 MeV and 240 MeV. Extracted OM parameters are listed in Table 2**.** Again, it is evident from Table. 2 that with increase of incident beam energy, real depth decreases whereas imaginary depth increases for a certain low energy range provided the fact that radius and diffuseness parameters are kept fixed in that energy range.

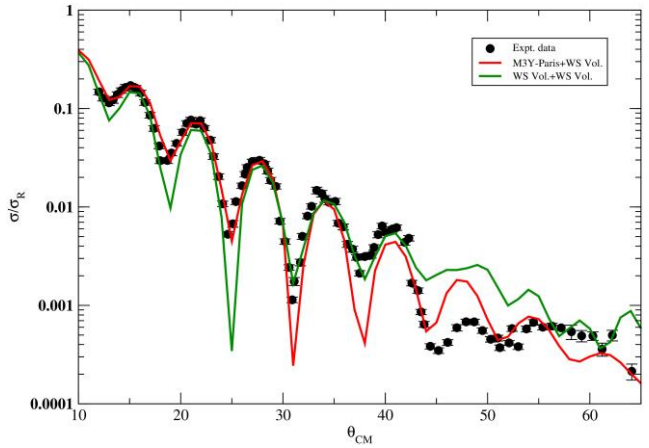

Fig. 4 The elastic scattering angular distribution of ^{6}Li+^{40}Ca reaction at 88 MeV using BDM3Y-Paris and WS potentials are compared with the experimental data. In the plot, black dots are experimental data points. Experimental data are taken from [18]

The elastic scattering angular distribution of ^{6}Li+^{40}Ca at energy of 20 MeV has been carried out using the two OM approaches as discussed above and the result is given as comparison with experimental data in Fig. 1. In the first approach, experimental cross sections are reproduced with N_R = 1.45 and the imaginary parameters are W_0 = 30 MeV, r_{0I} = 1.1 fm and a_{0I} = 0.65 fm. Bethge *et al.* extracted the OM parameters for ^{6}Li+^{40}Ca at energy of 20 MeV using WS potential and found that real WS volume parameters are V_0 = 32.6, r_{0R} = 1.18 fm and a_{0I} = 0.64 and the corresponding imaginary parameters are 7.4 MeV, 1.71 fm and 1.0 fm respectively [15]. Moreover, Bethge *et al.* assumed the Coulomb radius parameter to be 2.5 fm. In our second approach, WS depth parameters are 123 MeV and 35 MeV respectively for both real and imaginary parts. Radius and diffuseness parameters are 1.1 fm and 0.63 fm respectively and are same for both real and imaginary parts of the potential. Both the approaches produce experimental angular distribution quite satisfactorily.

Next we have analyzed the elastic scattering cross section for ^{6}Li+^{40}Ca at energy 26 MeV, 28 MeV, 30 MeV and 34 MeV. Previously, Cook *et al.* has analyzed for this system at the mentioned energies using a real M3Y potential and an imaginary WS volume potential [16]. In their analysis, N_R has variation in between 0.63 and 0.64, whereas imaginary depth has gradual increment from 9.63 MeV to 11.06 MeV with increase of energy of ^{6}Li. For 26 MeV, they found that N_R=0.65, W_0=9.63 MeV, r_{0I}=1.99 fm and a_{0I}=0.69 fm. Data obtained by using the DF+WS potential fit to the experimental data for $\Theta<90^0$. Compared to the data obtained by Cook *et al.*, our data obtained from the model constructed with DF and WS potential shows good agreement at angle more than 90^0 with the parameters N_R=1.36, W_0=39 MeV, r_{0I}=1.1 fm and

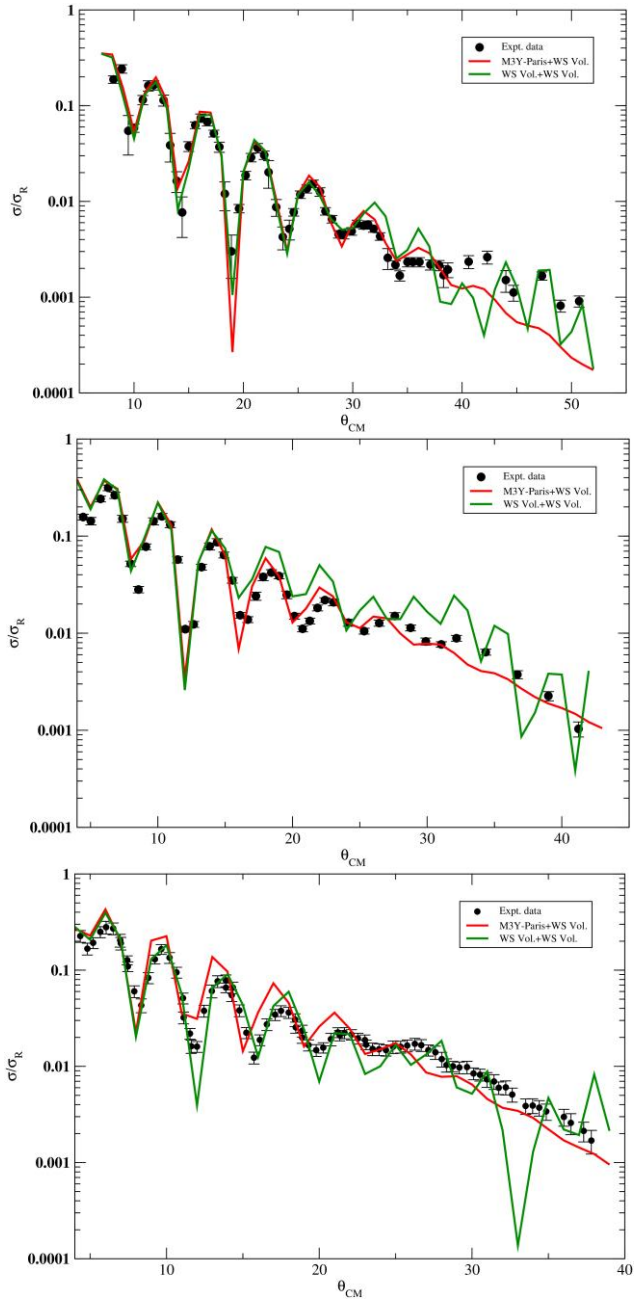

Fig. 6 The elastic scattering angular distribution of ^{6}Li+^{40}Ca reaction at 156 MeV (top), 210 MeV (middle) and 240 MeV (bottom) using BDM3Y-Paris and WS potentials are compared with the experimental data. In the plot, black dots are experimental data points. Experimental data are taken from [20-22]

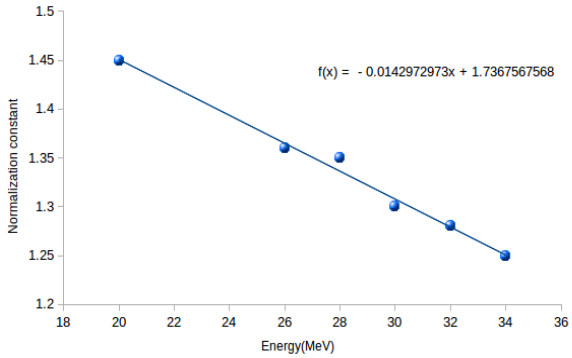

Fig. 7 Variation of normalization constant (N_R) of DF potential with beam energy

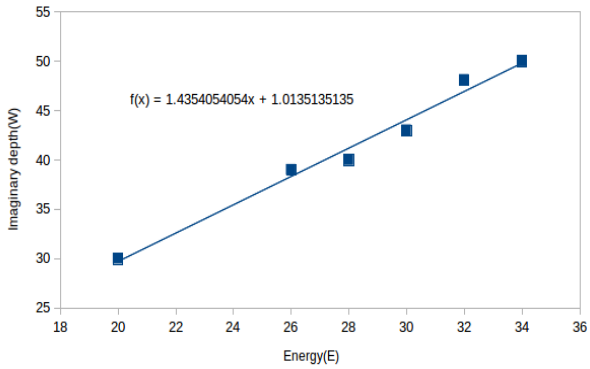

Fig. 8 Variation of imaginary WS Volume depth (for the first model) with beam energy

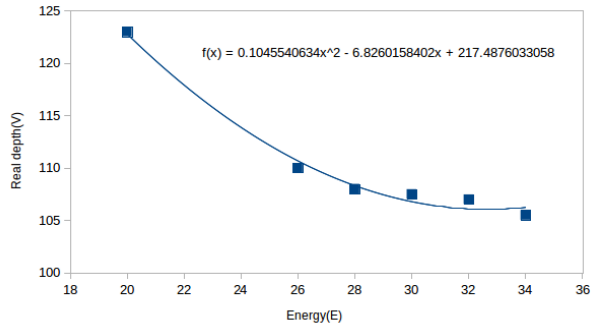

Fig. 9 Variation of real WS volume depth (V_0) with beam energy

a_{0I}=0.65 fm. However, data obtained with the second approach do not agree with experimental angular distribution above 90^0 (Fig. 2). Similarly, at other energies OM parameters are extracted by using the two approaches as described in Sec. II. Here, we present the extracted OM parameters by Cook *et al.* along with our data in Table 3. Both sets of parameters are found to be quite good in extracting experimental angular cross section and it is evident that certain parameters can be kept fixed for small energy difference. However, a question arise regarding the usefulness of radius parameter of around 2 fm in case of projectiles like ^{6}Li as done by Cook *et al.* though the present nuclear scattering analysis has set a boundary for radius parameter to be at around 1.1 fm to 1.4 fm. Moreover, it is desirable to consider r_0 to be around 1.1-1.3 fm for nearly spherical projectile like ^{6}Li which is incorporated in the present study.

From Table 3, it is clear that N_R decreases with increase of incident energy and imaginary depth shows opposite nature when radius and diffuseness parameters are kept fixed. In our approach we have kept fixed two parameters - r_{0I} and a_{0I}. OM parameters obtained by Cook *et al.* fail to reproduce experimental cross section above 90^0. However, our model with BDM3Y-Paris potential shows improvement at large angle cross section. The OM parameters extracted using the second approach is already listed in Table 2. Agreement with the experimental data is more likely in the first approach. However, both approaches fail to fit the experimental angular distribution above 60^0 at energy of 34 MeV. In Fig. 2, angular

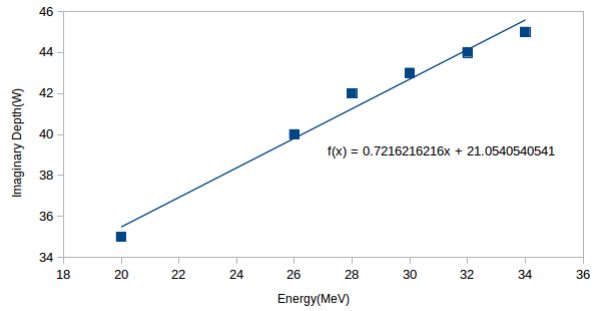

Fig. 10 Variation of imaginary WS volume depth (W_0) with beam energy for the second approach.

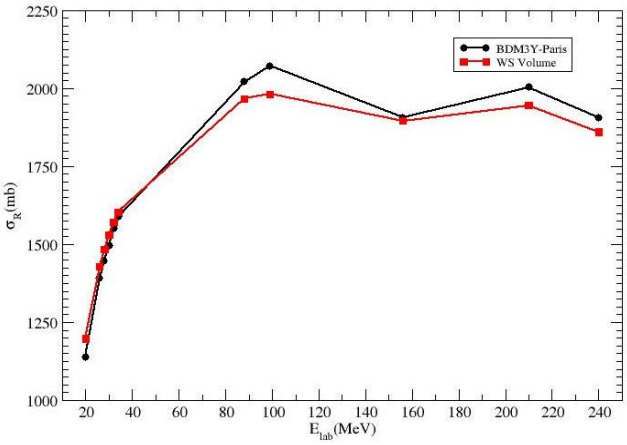

Fig. 11 Excitation functions for elastic scattering of ^{6}Li+^{40}Ca. The black line indicates cross section found using real BDM3Y-Paris potential whereas the red line is for real WS Volume potential.

distributions at energies 28 MeV, 30 MeV and 34 MeV are shown. At energies 28 MeV and 30 MeV, theoretical cross section fits with the experimental cross section with a great extent.

One striking remark from the analysis at 26 MeV and 34 MeV is that large angle anomaly. Large angle anomaly is thought to be a consequence of weak absorption that leads the dependence of scattering on interacting nuclear potential. DF potential is quite effective in producing experimental cross sections at large angles.

Another OM parameters extraction was carried out at 32 MeV (Fig. 3). Anantaraman *et al.* tried to fit the data with the OM parameters extracted previously by Chua *et al.* for ^{6}Li+^{40}Ca at energy of 50.6 MeV [17, 36]. Later on modifications were done in Chua potential in order to fit the data. In our first experimental cross-section shows good agreement with experimental data when analysis is carried out with the parameters: N_R=1.28, W_0=48.1 MeV, r_{0I}=1.1 fm and a_{0I}=0.65 fm. However, fitting process does not go well with the second approach. Best fit data are obtained with the parameters: V_0=107 MeV, r_{0R}=1.1 fm, a_{0R}=0.63 fm, W_0=45 MeV, r_{0I}=1.1 fm, a_{0I}=0.63 fm.

At very high energy, the experimental data show pronounced oscillations at smaller angles (above 10^0) but dies out with increasing angle and with increasing energy. Data along with our present analysis of elastic scattering angular distribution for ^{6}Li+^{40}Ca at energies 156 MeV, 210 MeV and 240 MeV are shown in Fig. 6. Calculations with BDM3Y-Paris (for real part) and WS volume term (for imaginary potential) reproduces experimental data quite satisfactory at these energies. However the OM calculations with WS potential (for both the real and imaginary part of the potential) though give reasonable good agreement with measured data at smaller angles ($\Theta_{CM}<20^0$) but failed to failed to describe at larger angles (our analysis is limited upto angle 40^0). At beam energy of 156 MeV, normalization constant used is N_R=0.90 and varies to 1.1 for energies 210 MeV and 240 MeV. Radius parameter is fixed at 1.0 fm whereas diffuseness parameter has variation from 0.884 fm to 0.811 fm for 210 MeV and 240 MeV respectively. In the second approach, both real and imaginary part of WS potential depths are varied along with the diffuseness and radius parameters as given in Table. 2. This model fails to reproduce experimental angular distribution beyond 20^0.

From the above study, we have extracted new set of OM parameters for ^{6}Li+^{40}Ca. Out of the two models DF model is found to be more effective in reproducing experimental data at low to very higher energy. However, WS formalism fails to produce data at energies above 156 MeV. This may be due to exclusion of explicit overlap of density profiles of colliding nuclei in this model. Also spin-orbit interaction part is completely ignored in this analysis though ^{6}Li has spin of +1. Moreover, with increase of beam energy, more and more non-elastic channels like transfer, fusion etc. open up due to penetration of incoming beam. We focus this study to extract correlations among various OM parameters at low energies.

The OM analysis provides approximate correlation among different combination of parameters. Fig. 7 and Fig. 8 show that real N_R decreases with beam energy whereas imaginary WS depth increases with beam energy when radius and diffuseness parameters are kept fixed at 1.1 fm and 0.63 fm over the energy range of 20 MeV-34 MeV. These variations indicate that absorption of incoming flux becomes prominent with increase of incident beam energy. In the plots, trend lines are shown and approximate trend line equations are determined. This trend line equations may provide a tool to extract OM parameters at any energy in the range 20MeV-34 MeV. The approximate variation of N_R with E_{Lab} is $N_R = -0.014E_{Lab}+1.74$ whereas W_0 varies as $W_0 = 1.435E_{Lab}+1.014$.

Similarly, variation of real as well as imaginary depth of WS Volume potential of second model are observed with the variation of beam energy keeping the radius and diffuseness parameters fixed over the energy range 20 MeV to 34 MeV. Real depth decreases with increase of energy whereas imaginary depth increases with increase of energy (Fig. 9 and Fig. 10) indicating more absorption of incident flux at higher energies. Approximate trend lines for these two variations are also determined and found that real WS depth follows a second order polynomial variation with beam energy as $V_0 = 0.104E_{Lab}^2 - 6.826E_{Lab}+217.488$ whereas imaginary WS depth increases linearly with energy as $W_0 = 0.723E_{Lab}+21.054$.. However, similar trends are not observed for the energy range 88 MeV – 240 MeV as variation of OM parameters is not systematic due to large energy difference.

TABLE II. OM PARAMETERS ARE EXTRACTED FROM ELASTIC SCATTERING ANALYSIS OF ^{6}LI+^{40}CA AT VARIOUS BEAM ENERGIES. BOTH REAL AND IMAGINARY PARTS OF THE NUCLEAR POTENTIAL HAVE WOOD-SAXON VOLUME FORM

Energy (MeV)	V_0 (MeV)	r_{0R} (fm)	a_{0R} (fm)	W_0 (MeV)	r_{0I} (fm)	a_{0I} (fm)	Type (WS)
20	123	1.1	0.63	35	1.1	0.63	Volume+Volume
26	110	1.1	0.63	40	1.1	0.63	Volume+Volume
28	108	1.1	0.63	42	1.1	0.63	Volume+Volume
30	107.5	1.1	0.63	44	1.1	0.63	Volume+Volume
32	107	1.1	0.63	45	1.1	0.63	Volume+Volume
34	105.5	1.1	0.63	46.24	1.1	0.63	Volume+Volume
88	109.5	0.884	0.865	46.24	1.0	0.865	Volume+Volume
99	109.5	0.865	0.811	57	1.001	0.840	Volume+Volume
156	110	0.884	0.811	55	1.0	0.811	Volume+Volume
210	95.0	0.965	0.760	55	0.990	0.885	Volume+Volume
240	109.5	0.865	0.811	46.24	1.001	0.881	Volume+Volume

TABLE III. OM PARAMETERS EXTRACTED FOR ^{6}LI+^{40}CA AT ENERGIES 26 MEV, 28 MEV, 30 MEV AND 34 MEV BY COOK *ET AL.* ARE LISTED ALONG WITH THE PARAMETERS OBTAINED FROM THIS WORK. COOK *ET AL.* USED A REAL DF POTENTIAL AND IMAGINARY WS POTENTIAL IN THIS ANALYSIS AND WE HAVE CARRIED OUT THE ANALYSIS CONSIDERING BDM3Y-PARIS POTENTIAL.

Energy (MeV)	Cook *et al.*				This Work			
	N_R	W_0 (MeV)	r_{0I} (fm)	a_{0I} (fm)	N_R	W_0 (MeV)	r_{0I} (fm)	a_{0I} (fm)
26	0.65	9.63	1.99	0.69	1.36	39	1.1	0.65
28	0.65	11.24	1.98	0.75	1.35	40	1.1	0.65
30	0.63	10.01	1.97	0.68	1.30	43	1.1	0.65
34	0.64	11.06	1.94	0.73	1.25	50	1.1	0.65

In this process of OM parameters extraction, we have also evaluated reaction cross section (σ_R) for the two models as mentioned above. Excitation function for elastic scattering of ^{6}Li from ^{40}Ca shows that with increase of beam energy cross section increased gradually and then it remains almost flat over the range 80 MeV – 240 MeV as plotted in Fig. 11. Cross section found using a real WS volume potential is found to underestimate the result obtained using BDM3Y-Paris potential. At energy above 156 MeV, potential becomes almost insensitive to the depth parameter; rather it depends on the geometry of the colliding nuclei. From 20 MeV to 34 MeV, cross section increases linearly with the increase of beam energy.

IV. CONCLUSION

In this work, we have carried out elastic scattering analysis of ^{6}Li+^{40}Ca at eleven energy points using two OM approach. In the first approach, real part of nuclear potential is taken to be BDM3Y-Paris potential whereas the imaginary part is taken to have WS volume formalism. In the second method, both real and imaginary parts are WS volume type. Using these two methods, new set of OM parameters are extracted. In the first approach using BDM3Y-Paris, normalization factor decreases roughly with increase of beam energy from 20 MeV to 34 MeV. As well, imaginary depth increases from 30 MeV to 50 MeV with the increase beam energy from 20 MeV to 34 MeV. It is observed that elastic scattering data of ^{6}Li is sensitive to the potential near the strong absorption radius ($1.3(A_P^{1/3}+A_T^{1/3})$ fm). Overlap of densities takes place because of which large angle anomalies are observed. In the second approach, real depth decreases with increase of beam energy whereas imaginary depth increases gradually. At higher energies in the range 150 MeV - 240 MeV, oscillation in angular distribution is prominent and also it is observed that peaks occur at very small scattering angle (around 10^0). In this energy range, OM analysis using WS potential does not produce experimental data above scattering angle 20^0 satisfactorily, and therefore, analysis is carried out using DF potential considering BDM3Y-Paris as a candidate. Calculation using DF potential produces best fit data at small scattering angles.

Though spin terms are less important for determining cross section, however omission of spin +1 of ^{6}Li is not justified properly in this study as the codes used do not provide option to include the same. Data around 30 MeV have shown anomalous angular behavior which may reveal more about the potentials at smaller distances. However, modifications in the DF potential is required injecting the concepts like L - dependence or surface transparency in order to explain low energy weak absorption properly. Though, the DF potential works on G-matrix calculation for scattering analysis, however, it is more desirable to introduce explicit energy dependence term so that at energy above 100 MeV this model can be applied satisfactorily. For that T-matrix interaction should be included.

In the present analysis we observed that calculations with WS potential somehow do not give a good agreement with the measured data at higher energy (above 156 MeV). Opening of more non-elastic channel at higher energy leads that WS formalism is not adequate for scattering analysis. The measured data show smooth angular dependence at angle $\Theta_{CM} > \sim 25^{0}$, in contrast, the present calculations show oscillatory nature. This needs further investigation which is beyond the scope of this work. Both models can be used satisfactorily at low energies and the OM parameters extracted can be used as a powerful tool in theoretical and experimental studies of ^{6}Li induced nuclear interactions. The approximate trend line equations provide an opportunity to extract the OM parameters for the both models in the energy range 20-34 MeV.

ACKNOWLEDGMENT

The authors are very much thankful to the funding agency Department of Atomic Energy-Board of Research in Nuclear Science (DAE-BRNS), Mumbai, India for providing financial grant to carry out this work under the project (Ref. No: 37(3)/14/09/2018-BRNS/37135 dated 05/07/2018).

REFERENCES

[1] Zhang Gao-Long, Zhang Huan- Qino, Liu Zu-Hua *et al.*, High Energy Physics and Nuclear Physics, Vol. 31, No. 7, July, 2007
[2] M. Aygun, Ann. Nucl. Energy 51 (2013) 1
[3] M. Aygun, Y. Kucuk, I. Boztosun and Awad A. Ibraheem, Nucl. Phys. A 848 (2010) 245
[4] M. Aygun, Commun. Theor. Phys. 60 (2013) 69
[5] N. Burtebeav, M. K. Baktybeav, B.A. Duisebeav, R.J. Peterson and S.B. Sakuta, Phys. At. Nucl. 68 (2005) 1303
[6] D.L. Pham, Journal de Physique Letters 37 (1976) 67
[7] A.T. Rudchik *et al.*, Nucl. Phys. A 939 (2015) 112
[8] S. Watanabe, Nucl. Phys. 8 (1958) 484
[9] G.R. Satchler, W.G. Love, Phys. Rep. 55 (1979) 183
[10] M.E. Brandan, G.R. Satchler, Phys. Rep. 285 (1997) 143
[11] G. Bertsch, J. Borysowicz, H. McManus, W.G. Love, Nucl. Phys. A284 (1977) 399
[12] N. Anantaraman, H. Toki, G.F. Bertsch, Nucl. Phys. A398 (1983) 269
[13] M. Hemalatha, PRAMANA-journal of physics, Vol. 82, No. 5, May 2014, pp.789-795
[14] C.L. Woods, B.A. Brown, N.A. Jelley; J. Phys. G: Nucl. Phys. 8(1982) 1699-1719
[15] K.Bethge, C.M.Fou, R.W.Zurmuhle, Nuclear Physics, A123 (1969) 521-530
[16] J. Cook, K.W. Kemper, M.F. Vineyard, Physical Review, C26 (1982) 486-492
[17] N. Anantaraman, H.W. Fulbright, P.M. Stwertka, Physical Review, C22 (1980) 501
[18] C.B. Fulmer, G.R. Satchler, E.E. Gross, F.E. Bertrand, C.D. Goodman, D.C. Hensley, J.R. Wu, N.M. Clarke, M.F. Steeden, Nuclear Physics, A356 (1981) 235
[19] P.Schwandt, W.W.Jacobs, M.D.Kaitchuck, P.P.Singh, W.O.Ploughe, F.D.Becchetti and J.Janecke, Physical Review, C24 (1981) 1522
[20] J. Cook, H. J. Gils, H. Rebel, Z. Majka, H. Klewe-Nebenius, Nuclear Physics, A388 (1982) 173-186
[21] A. Nadasen, M. McMaster, M. Fingal, J. Tavormina, P. Schwandt, J.S. Winfield, M.F. Mohar, F.D. Becchetti, J.W. Janecke, R.E. Warner, Physical Review, C39 (1989) 536-545
[22] Krishichayan, X. Chen, Y.-W. Lui, J. Button, D. H. Youngblood, Physical Review, C81 (2010) 044612
[23] http://nrv.jinr.ru/nrv/webnrv/elastic_scattering/els1.htm
[24] M.E. Brandan, M.S. Hussein, K.W. McVoy and G.R. Satchler, Comments Nucl. Part. Phys. 22, 77 (1996)
[25] P. Hodgson, The optical model of Elastic Scattering, Oxford Univ. Press, London, 1963
[26] R.C. Fuller, Phys. Rev. C12 (1975)1561
[27] R. Bass, Nuclear Reactions with Heavy Ions, Springer-Verlag, Berlin, Heidelberg, 1980
[28] M.S. Hussein, K.W. McVoy, Progr. Part. Nucl.Phys.,12 (1984) 103
[29] J.P. Jeukenne, A. Lejenue and C. Mahaux, Phys. Rev. C 16, 80 (1977)
[30] A.M. Kobos, B.A. Brown, P.E. Hodgson, G.R. Satchler and A. Budzanowski, Nucl. Phys. A384, 65 (1982)
[31] A.M. Kobos, B.A. Brown, R. Lindsay and G.R. Satchler, Nucl. Phys. A425, 205 (1984)
[32] G.R. Satchler and W.G. Love, Physics Reports 55 (1979) 183
[33] M.E. Brandan and G.R. Satchler; Physics Reports 285 (1997) 143-243
[34] H. De Vries, C.W. De Jager and C. De Vries; Atomic Data and Nuclear Data Tables 36 (1987) 495-536
[35] Dao T. Khoa and W. von Oertzen; Physics Letters B304 (1993) 8
[36] Dao T. Khoa, G. R. Satchler and W. von Oertzen; Physical Review C56 (1997) 954
[37] L.T. Chua, F.D. Becchetti, J. Janecke and F. L. Milder; Nuclear Physics A273(1976) 243-252